arXiv:1402.6070v1 [cond-mat.mtrl-sci] 25 Feb 2014

Enhanced optical properties and the origin of carriers transport in $BiFeO_3/TiO_2$ heterostructures with 109° domain walls

Hong-Jian Feng[a],* Bi Duan[a], Feng Liu[b], Jinshou Tian[b], and Xiaohui Guo[b]
[a] *School of Physics, State Key Laboratory of Photoelectric Technology and Functional Materials (Cultivation Base), Northwest University, Xi'an 710069, People's Republic of China and*
[b] *State Key Laboratory of Transient Optics and Photonics, Xi'an Institute of Optics and Precision Mechanics, CAS, Xi'an 710119,People's Republic of China*

The absorption performance in the $BiFeO_3/TiO_2$ bilayer film prepared by simple sol-gel method has been significantly improved in the ultraviolet and visible-light region, comparing with $BiFeO_3$ and TiO_2 films. Terahertz-radiation emission presents a direct evidence of photon-induced electrons and holes transport in the heterostructures. First-principles calculations agree well with the experiments and present an unambiguous explanation of charge carriers transport and enhanced absorbance which is induced by the large electrostatic potential drop in the interface of heterostructures with the 109° domain walls. This work provides a promising candidate toward designing novel photovoltaic $BiFeO_3$-based heterostructures with high efficiencies.

PACS numbers: 73.61.-r, 75.70.-i, 71.15.Mb

Multiferroic $BiFeO_3$(BFO) has attracted much interests due to its coexistence of antiferromagnetic(AFM) and ferroelectric(FE) ordering at room temperature[1, 2]. This permits the tunable magnetization by electric field owing to the coupling between FE displacement along the eight pseudocubic [111] diagonal directions and the G-type AFM plane, and vise versa[3, 4]. As the spin cycloid is suppressed in thin films ,heterostrutures composed of BFO thin films have been proposed to implement ferromagnetic(FM) reversal controlled by electric field via the exchange bias coupling between the AFM-FM interface, which can be used in the spintronics and information storage field[5, 6]. Recently, the photovoltaic(PV) properties observed in BFO makes it an excellent candidate for application in solar cells due to its relatively small band gap of 2.67 eV[7]. Regarding the depletion layer of micrometer-thick in Schottky barrier, the ferroelectric domain walls of BFO with thickness of only 1-2 nm is able to separate the electrons and holes and drive the large photovoltage and PV performance[8]. Periodically ordered domain walls in pure BFO samples with excellent PV performance have been prepared[9, 10], and the photovoltages measured are additive and the resultant voltages are much larger than the band gap[11]. Experiments demonstrate that the bulk photovoltaic effect (BPVE) plays a crucial role in the PV properties in BFO thin films[12], and the dominant mechanism of the BPVE in ferroelectrics is still under debate[13]. Density functional theory(DFT)-based *ab initio* calculations indicate that the BPVE plays a role and interacts cooperatively with the domain-wall-driven voltages in polydomain BFO samples[14].This ferroelectrics-based BPVE makes BFO a prospective candidate for manufacturing solar cells with higher photovoltage and energy efficiency. As expected, the enhanced PV properties have been observed in graphene/polycrystalline BFO/Pt heterostructures[15],and we suggest the coupling effect in the interface is associated with the interaction between photon, carrier, charge, and spin. Can the optical behavior be improved in other BFO-based heterojunctions? What is the origin of the enhanced absorbance and PV effect? Can we present some direct evidences for the photon-induced charge carriers transport in it?

Owning to the stronger absorption in surface, anatase TiO_2(TO) is well known as a promising candidate for photocatalyst and nanostructured solar cells [16, 17]. As demonstrated in our previous study[18], Ti in B-site doped BFO plays a crucial role in stabilizing the ferroelectricity and insulating properties in BFO samples[19]. Hereby, BFO/TO bilayer films are expected to perform magneto-optic, electro-optic,and magnetoelectric coupling effect in the interface and carriers transfer properties as discussed in our preceding work[20, 21]. In addition, the ferroelectric domain walls[8], as well as the asymmetry in heterostructures, would drive separation of photon-induced carriers and result in an improved PV response. In this Letter,we prepared BFO/TO bilayer films using sol-gel method, and as expected an improved absorbance has been observed in the heterojunctions. The terahertz(THz) time domain wave form have been carried out to witness the occurrence of photon-induced carriers transport owing to its ability of detecting the charge carriers transport in BFO [22]and the organic ferroelectrics[23]. DFT based first-principles calculations agree well with the experimental results and present an unambiguous explanation for the increasing optical response in the hetereostructures.

The BFO sols were prepared using iron nitrate, bismuth nitrate, and acetic acid as the solutes and 2-methoxyethanol as the solution. The solution was adjusted to a pH value of 4-5 by adding nitric acid. Then citric acid in 1:1 molar ratio with respect to the metal nitrates was added to the solution as a complexant. The mixture was stirred for 24 hours to obtain the sol.The

* Email: hjfeng@nwu.edu.cn, fenghongjian@gmail.com

final concentration of the precursor was 0.3 mol/l. The films were spin coated on glass slide substrates in terms of its cost-effective application. After each spin coating, the films were dried at 80 °C for 2 hours. The obtained films were annealed at 500 °C in the air for 3 hours. The thickness of the films could be controlled by the number of layers spin coated. The precursor solution of TO was prepared by mixing appropriate amounts of tetrabutyl titanate dissolved in ethanol, and diethanolameine was dropwise added into the solution stirring for 2 hours. The TO films were spin coated on the BFO films and calcined at 500 °C for 1 hour with the thickness of the films controlled by different layers coated.

The structure and morphology of the BFO and BFO/TO films were investigated by X-ray diffraction (XRD)(Bruker D8 Advance).The ultraviolet (UV)-vis absorption spectra were measured on a UV-vis spectrophotometer (PerkinElmer Lambda 950) with deuterium and tungsten-halogen lamp as illuminant. The wavelength is varying from 200 to 800 nm. The BFO films and heterostructures were tested on a typical transmission THz time domain spectroscopy (THz-TDS) system. Femtosecond laser pulses with wavelength of 800 nm, pulse duration of 69 fs, repetition rate of 80 MHz, and average power of 200 mW illuminate on a photoconductor antenna emitter. The generated THz pulse with pulse duration of 2 ps and spectrum range of 1.5 THz transmitted through the samples, and optically sampled in a ZnTe receiver with thickness of 2 mm.

XRD patterns for BFO film(1μm) and BFO(1μm)/TO(100nm) heterostructure are shown in Fig. 1(b). All diffraction peaks can be indexed according to the standard powder diffraction data of BFO , indicating the single perovskite phase of BFO film. The (1 0 1) and (2 0 0) peaks found in the bilayer film are attributed to the anatase TO. The experimental absorption spectrum for BFO-based films are reported in Fig.2 (a). It is clear that in the visible-light region the absorption coefficient is increased significantly in BFO/TO bilayer film, comparing with that in BFO and TO films. The bilayer film also exhibits a better optical performance in the near UV region implying that BFO/TO heterostructure is an ideal candidate for PV applications in the wavelength ranging from 300 to 800 nm.

In addition, first-principles calculations have been carried out to confirm the experiments and present an unambiguous understanding for the improved optical behaviors. We used the local spin density approximation(LSDA) to DFT scheme with an uniform energy cutoff of 500 eV as in our previous work [21, 24]. We considered Bi 5s, 5p, and 6s electrons, Fe 3s, 3p, and 3d electrons,Ti 3s, 3p, and 3d and O 2s and 2p electrons as valence states. $6 \times 6 \times 1$ Monkhorst-Pack sampling of the Brillouin zone were chosen for the relaxation process while they were increased to $20 \times 20 \times 1$ to insure the convergence for the total energy calculation. We used the slab model to construct (0 0 1) surface for the bilayer films while a same vacuum thickness was constructed to avoid the influence caused by the periodic boundary condition. The relaxation were carried out as the forces on the ions were less than 0.02 meV/Å. We introduced the on-site Coulomb interaction by adding a Hubbard-like term to the effective potential in that DFT+U scheme can describe precisely an appropriate band gap for the strongly correlated transition metal oxides[25–27], and it is susceptible to the Dzyaloshinskii-Moriya interaction(DMI)[28, 29] and consequently the absorption spectrum.

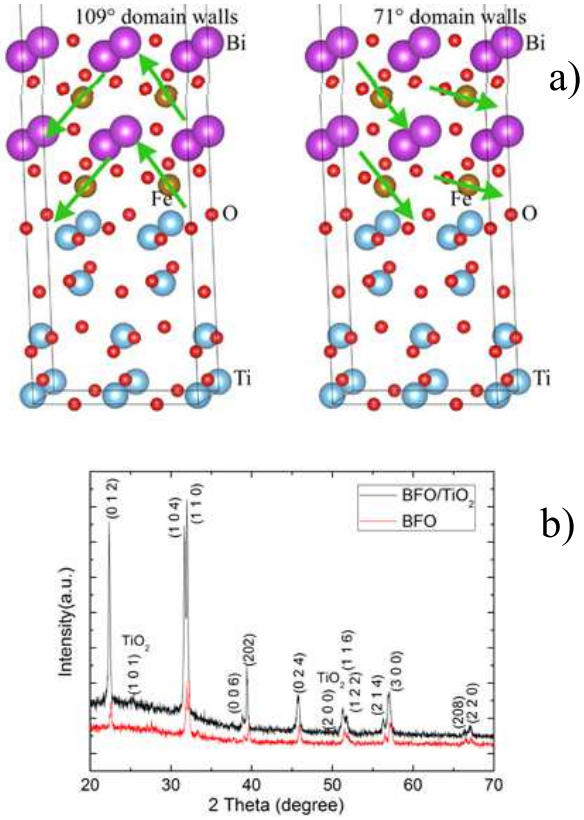

FIG. 1. (a)71° and 109° domain structures.(b)XRD patterns for BFO and BFO/TO bilayer film.

In terms of calculating the optical spectra, the imaginary part of the dielectric tensor is determined by the summation over the conduction band states[30]

$$\varepsilon''_{ij}(\omega) = \frac{4\pi^2 e^2}{\Omega} \lim_{q\to 0} \frac{1}{q^2} \sum_{c,v,k} 2w_{\mathbf{k}} \delta(\varepsilon_{c\mathbf{k}} - \varepsilon_{v\mathbf{k}} - \omega) \times \\ < u_{c\mathbf{k}+e_i\mathbf{q}} | u_{v\mathbf{k}} > < u_{c\mathbf{k}+e_j\mathbf{q}} | u_{v\mathbf{k}} >^*, \quad (1)$$

where c and v denote the conduction and valence band states, respectively. Kramers-Kronig transformation is used to derive the real part of the dielectric tensor

$$\varepsilon'_{ij}(\omega) = 1 + \frac{2}{\pi} P \int_0^\infty \frac{\varepsilon''_{ij}(\omega')\omega'}{\omega'^2 - \omega^2 + i\eta} d\omega'. \quad (2)$$

The corresponding absorption spectrum was obtained by

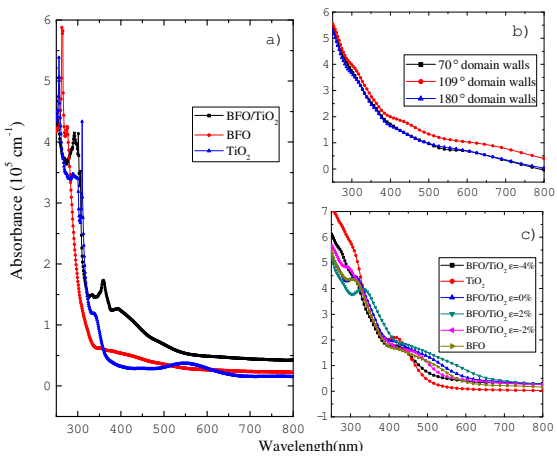

FIG. 2. (a)The optical absorption curves for BFO-based films. (b)Calculated absorption spectra for different domain walls in BFO/TO heterostructures.(c)Calculated absorption spectra for BFO, TO, and BFO/TO heterostructure under different strains.

the following expression:

$$I(\omega) = 2\omega \left(\frac{(\varepsilon'^2(\omega) + \varepsilon''^2(\omega))^{1/2} - \varepsilon'(\omega)}{2} \right)^{1/2}, \quad (3)$$

where I is the optical absorption coefficient, and ω is the angular frequency.

We construct the three kind of domain walls, namely 71°, 109°,and 180° domain walls[8], for BFO in the heterostructures, and the structure of 71° and 109° domain patterns are shown in Fig.1(a), while the polarization direction for 180° domain walls is changing from $[\bar{1}\ \bar{1}\ \bar{1}]$ to [1 1 1] and not shown in the graph. Firstly, we change the distance between Ti-O_2 and Fe-O_2 layers in the interface to find the stable structure, and then the strain, ϵ , is varied from -4% to 2%. Our theoretical results are illustrated in Fig. 2 (b),and (c), respectively. From Fig. 2 (c), one can see that the absorption performance of the heterostructures is superior to BFO and TO films as the strain is exerted from compression to tension, indicating the lattice mismatch and strain may exist in the samples as the theoretical results are in good agreement with the experiments. It is worth mentioning that the absorbance is increased significantly as the domain pattern changes from 71° or 180° to 109° while the former two patterns have nearly the same absorption curves. This accounts well for the agreement between calculations and experiments, showing the possibility of higher density of 109° domain walls in the BFO/TO bilayer films prepared.

The time domain wave form for BFO-based films are reported in Fig.3 (b), and the setup is shown in Fig. 3(a). The THz radiation is polarized from 0 to 90 degree to witness the anisotropic photon-induced electrons and holes pairs transport. It can be seen that the peak amplitude for BFO/TO heterostructure is increased as the THz field is along 0 degree while the polarized direction

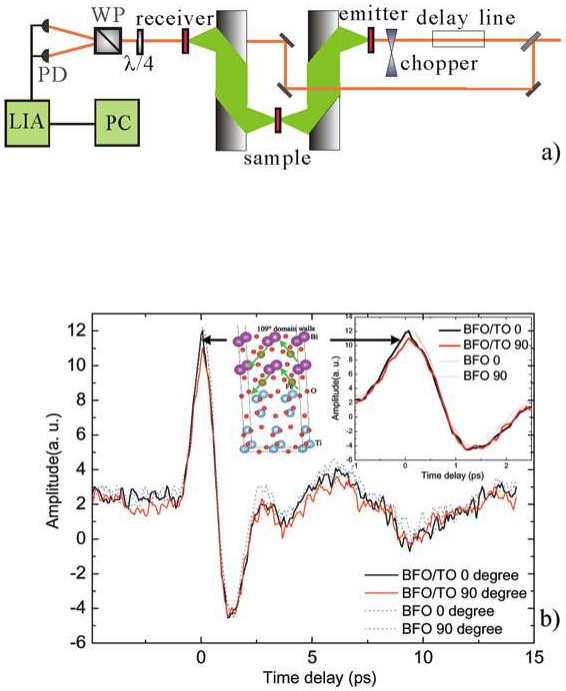

FIG. 3. THz emission measurements.(a) Schematic of setup. (b)Time evolution of emission for BFO-based films with 0 and 90 degree rotation, and the inset shows the expanded peak.

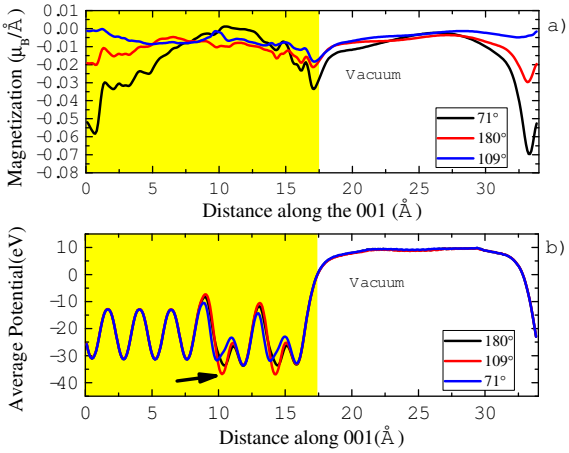

FIG. 4. (a)The distribution of spin density and (b)electrostatic potential across the bilayer film averaged over the plane parallel to the film for different domain patterns.

of THz has little influence on BFO film. This suggests the anisotropic properties of carriers transport and the corresponding improved absorption performance along a specific direction in the heterostructure, and the large absorbance is originating from the higher density of 109° domain walls along the direction.

In order to elucidate the separation and the transport of electrons and holes in the heterostructure, the plane-averaged spin density and electrostatic potential across

the film are shown in Fig. 4(a) and Fig.4(b), respectively. It is interesting that the averaged spin density for 109° domain pattern possess the lowest value, and this is understandable with the larger potential drop of about 5 eV across the interface in 109° domain structure while the other domain patterns only have potential drop of about 2 eV. The large potential drop is able to separate the photon-induced electrons and holes carriers to enhance the absorbance, and the large amount of carriers results in the decreasing of averaged spin density. The large potential drop in the interface can be caused by the interaction between the adjacent layers in the interface. Ti-O_2 layer is neutralized and Fe-O_2 layer is negatively charged. Therefore the different charged layers can create the higher potential difference. For 180° and 109° domain structures, the neighboring Fe ions displace in opposite directions perpendicular to the interface, leading to the higher potential drop than 71° domain. The condensation of Fe ions in plane makes the potential deviation in 109° domain patterns stronger than 180° structures. Eventually, the electrons and holes can be effectively separated by this large potential drop to create novel PV BFO-based heterostructures with high efficiencies.

In summary,BFO/TO heterojunction exhibits a stronger optical absorption than monolayer films, and theoretical calculations account well for the experiments with considering the 109° domain walls in the heterostructures. In addition 109° domain patterns can induce the large potential drop in the interface,leading to the higher density of photon-induced electrons and holes which is manifested by the THz time domain wave form.

ACKNOWLEDGMENTS

This work was financially supported by the National Natural Science Foundation of China(NSFC) under Grants No. 11304248 and No. 11247230(H.-J. F.), Scientific Research Program Funded by Shaanxi Provincial Education Department (Program No. 2013JK0624)(H.-J. F.), and the Science Foundation of Northwest University(Grant No. 12NW12)(H.-J. F.).

[1] J. Wang, J. B. Neaton, H. Zheng, V. Nagarajan, S. B. Ogale, B. Liu, D. Viehland, V. Vaithyanathan, D. G. Schlom, U. V. Waghmare, N. A. Spaldin, K. M. Rabe, M. Wuttig, and R. Ramesh, Science 299,1719 (2003).
[2] I.Sosnowskat,T.Peterlin-Neumaier, E. Steichele, J. Phys. C: Solid State Phys. 15, 4835 (1982)
[3] G. Catalan and J. F. Scott, Adv. Mater. 21, 2463 (2009)
[4] D. Lebeugle, D. Colson, A. Forget, M. Viret, A. M. Bataille, A. Gukasov, Phys. Rev. Lett. 100, 227602 (2008)
[5] H. Bea, M. Bibes, F. Ott, B. Dupe, X.-H. Zhu, S. Petit, S. Fusil, C. Deranlot, K. Bouzehouane, and A. Barthelemy,Phys. Rev. Lett. 100, 017204 (2008)
[6] A.Y. Borisevich, H. J. Chang, M. Huijben, M. P. Oxley, S. Okamoto, M. K. Niranjan, J. D. Burton, E.Y. Tsymbal, Y. H. Chu, P. Yu, R. Ramesh, S.V. Kalinin, and S. J. Pennycook, Phys. Rev. Lett. 105, 087204 (2010)
[7] S. R. Basu, L. W. Martin, Y.-H. Chu, M. Gajek, R. Ramesh, R. C. Rai, X. Xu, and J. L. Musfeldt, Appl. Phys. Lett. 92, 091905 (2008)
[8] S. Y. Yang, J. Seidel, S. J. Byrnes, P. Shafer, C.-H. Yang, M. D. Rossell, P. Yu, Y.-H. Chu, J. F. Scott, J.W. Ager, III, L. W. Martin and R. Ramesh, Nature Nanotech. 5, 143 (2010)
[9] T. Choi, S.Lee,Y. J. Choi,V.Kiryukhin, and S.W.Cheong, Science 324, 63 (2009)
[10] S. Y. Yang, L. W. Martin, S. J. Byrnes , T. E. Conry, S. R. Basu, D. Paran, L. Reichertz, J. Ihlefeld, C. Adamo, A. Melville, Y. H. Chu, C. H. Yang, J. L. Musfeldt, D. G. Schlom, J. W. Ager, and R. Ramesh, Appl. Phys. Lett. 95, 062909, (2009)
[11] J. Seidel, D. Fu, S. Y. Yang, E. Alarcon-Llado, J. Wu, R. Ramesh, and J. W. Ager III Phys. Rev. Lett. 107, 126805 (2011)
[12] W. Ji, K. Yao, and Y. C. Liang, Phys. Rev. B 84, 094115 (2011)
[13] S. M. Young and A. M. Rappe, Phys. Rev. Lett. 109, 116601 (2012)
[14] S. M. Young, F. Zheng, and A. M. Rappe, Phys. Rev. Lett. 109, 236601 (2012)
[15] Y. Zang, D. Xie, X. Wu, Y. Chen, Y. Lin, M. Li, H. Tian, X. Li, Z. Li, H. Zhu, T. Ren, and D. Plant, Appl. Phys. Lett. 99, 132904 (2011)
[16] A. Fujishima and K. Honda, Nature 238,37 (1972)
[17] Joseph Muscat, Varghese Swamy, and Nicholas M. Harrison, Phys. Rev. B, 65, 224112 (2002)
[18] H.-J. Feng, F. Liu, Phys.Lett.A, 372, 1904-1909 (2008)
[19] Y. Wang and C.-W. Nan, Appl. Phys. Lett. 89, 052903 (2006)
[20] H.-J. Feng, Physica B, 412, 41 (2013)
[21] H.-J. Feng, Europhys. Lett., 101, 67007 (2013)
[22] D. S. Rana, K. Takahashi, K. R. Mavani, I. Kawayama, H. Murakami, and M. Tonouchi, Phys. Rev. B, 77, 024105 (2008)
[23] T. Miyamoto1, H. Yada, H. Yamakawa, and H. Okamoto, Nature Commun. 4,2586 (2013)
[24] H.-J. Feng, J. Appl. Phys. 114, 123916 (2013)
[25] V.I. Anisimov, J. Zaane, O.K. Andersen, Phys. Rev. B, 44, 943(1991)
[26] V.I. Anisimov, I.V. Solovyev, M.A. Korotin, Phys. Rev. B 48, 16929(1993)
[27] V.I. Anisimov, F. Aryasetiawanz, A.I. Lichtenstein, J. Phys.: Condens. Matter, 9, 767(1997)
[28] H.-J. Feng, J. Magn. Magn. Mater., 322, 3755 (2010)
[29] H.-J. Feng, J. Magn. Magn. Mater., 324, 178 (2012)
[30] M. Gajdoš, K. Hummer, G. Kresse, J. Furthmüller, and F. Bechstedt, Phys. Rev. B, 73, 045112 (2006).